Electrical properties of n-amorphous/p-crystalline silicon heterojunctions

Hideharu Matsuura, Tetsuhiro Okuno,[a] Hideyo Okushi, and Kazunobu Tanaka
Electrotechnical Laboratory, 1-1-4 Umezono, Sakura-mura, Niihari-gun, Ibaraki 305, Japan

(Received 15 August 1983; accepted for publication 3 November 1983)

We have measured C-V characteristics and temperature dependence of J-V characteristics of undoped hydrogenated amorphous silicon (a-Si:H) heterojunctions formed on p-type crystalline silicon (p c-Si) substrates with different resistivities. It has been found that an abrupt heterojunction model is valid for a-Si:H/p c-Si heterojunctions, and the electron affinity of a-Si:H has been estimated as 3.93 ± 0.07 eV from C-V characteristics. The forward current of all the junctions studied shows voltage and temperature dependence expressed as $\exp(-\Delta E_{af}/kT)\exp(AV)$, where ΔE_{af} and A are constants independent of voltage and temperature, being successfully explained by a multitunneling capture-emission model. The reverse current is proportional to $\exp(-\Delta E_{ar}/kT)(V_D - V)^{1/2}$, where V_D is the diffusion voltage and ΔE_{ar} is a constant. This current is probably limited by generation-recombination process.

PACS numbers: 73.40.Lq, 73.60.Fw

I. INTRODUCTION

Single-crystalline heterojunctions have been extensively studied[1-6] from the viewpoints of understanding the fundamental device physics as well as their applications to many devices such as wide band-gap emitters,[7,8] majority carrier rectifiers,[1] high-speed wide bandpass photodetectors,[9] beam-of-light transistors,[10,11] indirect gap injection lasers,[12] and solar cells.[1] Amorphous heterojunctions might also be used for some of these applications, and, in fact, hydrogenated amorphous silicon carbide (a-SiC:H)/hydrogenated amorphous silicon (a-Si:H) solar cells have already shown a great potentiality.[13] However, the physics of amorphous heterojunctions is clearly far from being understood; even the amorphous homojunctions being not yet completely understood. The study of amorphous-crystalline heterojunctions can thus be a first step towards understanding amorphous-amorphous junctions.

Anderson,[1] Rediker *et al.*,[2] Hampshire *et al.*,[3] Riben *et al.*,[4,5] Donnelly *et al.*,[6] and other groups have reported the electrical properties of heterojunctions of crystalline materials. Anderson has initially proposed an energy band diagram assuming no interface states and extremely abrupt change from one material to the other. Rediker *et al.*,[2] Hampshire *et al.*,[3] and Riben *et al.*[4] reported the experimental evidences for supporting the abrupt heterojunction model (Anderson's model) through their C-V measurements. With regard to the current transport mechanism of heterojunctions, Anderson[1] and Perlman *et al.*[14] put the basis of their calculations on a Shockley diffusion model[15] and a Schottky emission model,[16] respectively, while Riben *et al.*,[4,5] Donnelly *et al.*,[6] and Rediker *et al.*[2] have independently published tunneling models to explain their own data.

On the other hand, there are very few reports concerning amorphous-crystalline heterojunctions after the first report of Grigorovici on a-Ge/c-Ge junction.[17] According to Štourač,[18] for the case of chalcogenide material, the junction is essentially approximated by the abrupt heterojunction and the current transport mechanism is based on the space-charge-limited currents in the amorphous material. Concerning a-Si:H crystalline heterojunctions, almost no data has been published so far.

In this paper, we present a systematic study of undoped (n^--type) a-Si:H/p-type crystalline silicon (p c-Si) heterojunctions for the first time. One of the purposes of this paper is to establish an energy band diagram of a-Si:H/c-Si heterojunctions, and the other is to elucidate the current transport mechanism of those heterojunctions.

II. EXPERIMENT

Undoped a-Si:H films were deposited by the glow discharge decomposition (GD) of pure SiH_4 on p c-Si (0.005–0.01, 0.1–0.15, 1–2, and 5–10 Ω cm) and n^+ c-Si(<0.02 Ω cm) substrates heated at 250 °C. Prior to a-Si:H deposition, silicon wafers were soaked in a solution of HF to remove SiO_2 and then rinsed in distilled water. A flow rate of 5 SCCM and a gas pressure of 50 mTorr were maintained during the deposition. Magnesium (Mg) was subsequently evaporated on an area of 0.785 mm^2 of the a-Si:H films in a vacuum of 7×10^{-7} Torr. Table I summarizes Mg/undoped a-Si:H/p c-Si diodes used in the present work, where a film thickness (L) of a-Si:H, the resistivity (ρ) and the density of acceptor impurities (N_A) of p c-Si are listed. N_A was determined by C-V measurements on Mg/p c-Si Schottky barrier diodes. The C-V characteristics of these diodes were measured at 100 kHz. The current-density versus voltage (J-V) characteristics were measured as a function of temperature in the range between 297 and 374 K in N_2 atmosphere. Any hysteresis effect was not observed in J-V characteristics when the diodes were heated up and cooled down cyclically.

III. RESULTS AND DISCUSSION

A. Mg/undoped a-Si:H contact

In order to investigate any properties of undoped a-Si:H/p c-Si heterojunctions, an ohmic contact has to be made with undoped a-Si:H. Although heavily P-doped a-Si:H (n^+ a-Si:H) forms an ohmic contact with undoped a-Si:H, the samples must be heated at around 300 °C when n^+ a-Si:H is deposited. This high temperature is likely to change

[a] On leave from Sharp Corporation, 2613-1 Ichinomoto-cho, Tenri-city, Nara 632, Japan.

 © 1984 American Institute of Physics

TABLE I. Various data of materials and diodes used in the present work. Experimental results obtained from *C-V* characteristics are also listed.

Sample number	*pc*-Si			Undoped *a*-Si:H						
	ρ (Ω cm)	N_A ($\times 10^{15}$ cm^{-3})	δ_1[a] (eV)	L (μm)	δ_2 (eV)	[b]	V_D (V)	N_I ($\times 10^{15}$ cm^{-3})	E_C (eV)	χ_2[c] (eV)
2	5–10	2.0	0.22	1.16	0.72	C	0.31	6.2	0.13	4.00
3	1–2	9.0	0.18	0.80	0.76	C	0.51	3.6	0.33	3.80
4	1–2	9.0	0.18	2.19	0.72	C	0.37	2.8	0.15	3.98
5	0.005–0.01	...	0	1.02	0.72	C	...	...	...	...
6	0.1–0.15	180	0.10	1.02	0.72	C	...	...	...	...
7	1–2	9.0	0.18	1.02	0.72	C	0.42	3.9	0.20	3.93
8	5–10	2.0	0.22	1.02	0.72	C	0.38	4.0	0.20	3.93
9	1–2	9.0	0.18	1.76	0.84	I	0.37	1.6	0.27	3.86
10	5–10	2.0	0.22	1.78	0.84	I	0.20	1.8	0.14	3.99

[a] $\delta_1 = kT\ln(N_V/N_A)$, $N_V = 1.02\times10^{19}$ cm^{-3} (Ref. 33).
[b] C: capacitively-coupled GD reaction chamber, I: inductively-coupled GD reaction chamber.
[c] χ_1 of 4.13 eV and E_{g1} of 1.12 eV (Ref. 33) are used to obtain χ_2.

the properties of the heterojunctions. This is one of the reasons why we use Mg for getting ohmic contact with undoped *a*-Si:H.[19] The Mg ohmic contact is as good as that obtained by using n^+ *a*-Si:H, which was previously described in comparison to the data of Wronski *et al.* using n^+ *a*-Si:H.[20] From *J-V* characteristics of the Mg/undoped *a*-Si:H/n^+ *c*-Si structure (sample 1) as shown in Fig. 1, it is clear that the Mg/undoped *a*-Si:H contact does not affect the *J-V* characteristics of the *a*-Si:H/*p* *c*-Si heterojunctions at each temperature, because the current level in the figure associated with Mg/undoped *a*-Si:H contact is higher than that of *a*-Si:H/*p* *c*-Si heterojunctions to be shown below.

B. Capacitance-voltage characteristics of undoped *a*-Si:H/*p* *c*-Si structure

C-V characteristics of the diodes were measured at 100 kHz. This frequency is high enough to be able to neglect a dielectric relaxation process in undoped *a*-Si:H (around 10^9 Ω cm in resistivity),[21,22] by which one can get information on the depletion layer extending in the *p* *c*-Si side regardless of that of the *a*-Si:H side. In fact, the capacitance of the diode (sample 5) using *p* *c*-Si (0.005–0.01 Ω cm) instead of *p* *c*-Si (1–2 and 5–10 Ω cm) measured at 100 kHz showed a constant value independent of applied voltage, coinciding with that of the capacitance determined only by the film dimension of *a*-Si:H, i.e.,

$$C = \frac{\epsilon_0 \epsilon_{s2}}{L}, \quad (1)$$

where ϵ_0 is the free space permittivity, ϵ_{s2} the dielectric constant of *a*-Si:H, and L the thickness of *a*-Si:H measured by Talystep. It clearly indicates that the measuring frequency is higher than the reciprocal of the dielectric relaxation time of undoped *a*-Si:H,[21,22] and besides, the depletion layer is negligibly thin in the side of *p* *c*-Si (0.005–0.01 Ω cm).

Figure 2 shows *C-V* characteristics of the sample 7 (*p* *c*-Si: 1–2 Ω cm). The capacitance level of the diode replaced by *p* *c*-Si of 0.005–0.01 Ω cm (sample 5) is also indicated in the

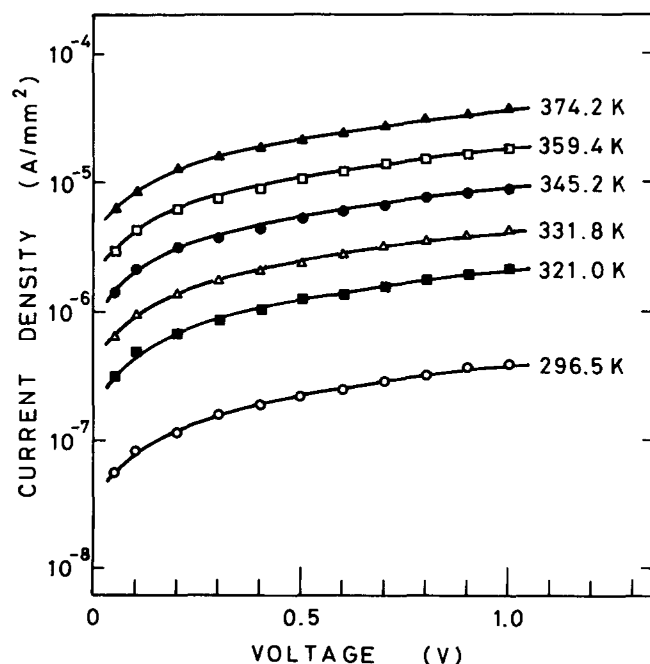

FIG. 1. *J-V* characteristics of Mg/undoped *a*-Si:H/n^+ *c*-Si diode (sample 1) measured at six different temperatures.

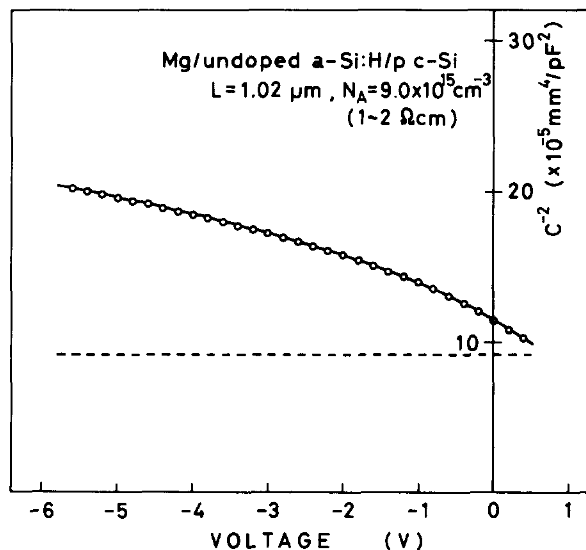

FIG. 2. C^{-2}-*V* characteristics of sample 7. The broken line is those of sample 5.

figure by a broken line. Different from the conventional C-V theory, as shown in the figure, $1/C^2$ is not proportional to the applied voltage.

The C-V characteristics in the figure is reasonably interpreted by assuming an ideal abrupt heterojunction without interface states. According to the abrupt heterojunction model, the present undoped a-Si:H/p c-Si heterojunction can be approximated by the energy band diagram as is shown in Fig. 3, although the model might originally be presented for the crystalline-crystalline heterojunction. χ is the electron affinity, V_D the diffusion voltage, δ the distance in energy from the Fermi level to the nearest band edge, E_g the energy band gap of the semiconductor, W the width of the depletion region, L the thickness of a-Si:H, ΔE the difference in energy between band edges of the two semiconductors, and ϕ_m the work function of Mg. The subscripts 1 and 2 refer to p c-Si and undoped a-Si:H, respectively, and the subscripts C and V refer to the conduction band and the valence band, respectively.

Since 100 kHz is much higher than the reciprocal of the dielectric relaxation time of undoped a-Si:H, the capacitance (C) measured at 100 kHz is generally expressed by the relation

$$\frac{1}{C}=\frac{W_1}{\epsilon_0\epsilon_{s1}}+\frac{L}{\epsilon_0\epsilon_{s2}}, \tag{2}$$

where W_1 and ϵ_{s1} are the width of the depletion region and the dielectric constant of p c-Si, respectively. Equation (2) can be simplified by the reasonable assumption of $\epsilon_{s1}\simeq\epsilon_{s2}$ into the following form:

$$C=\frac{\epsilon_0\epsilon_s}{L+W_1}. \tag{3}$$

According to the abrupt heterojunction model,[23]

$$\frac{V_{D1}-V_1}{V_{D2}-V_2}=\frac{N_I}{N_A} \tag{4}$$

and

$$W_1=\sqrt{\frac{2\epsilon_0\epsilon_s}{qN_A}(V_{D1}-V_1)} \tag{5}$$

are easily derived, where V_1 and V_2 are the applied bias voltages being supported in the depletion region in p c-Si and undoped a-Si:H, respectively, N_A the acceptor impurity density of p c-Si, N_I the effective density of localized gap states in a-Si:H and q the magnitude of electric charge. From Eqs. (3), (4), and (5), we get

$$W_1^2=\left(\frac{\epsilon_0\epsilon_s}{C}-L\right)^2$$
$$=\frac{2\epsilon_0\epsilon_s N_I}{qN_A(N_I+N_A)}(V_D-V). \tag{6}$$

Figure 4 shows W_1^2 vs $(V_D - V)$ relationship of the sample 7 (open circle), which was replotted from the data of Fig. 2. The data reveals quite a good linear relationship indicating that the abrupt heterojunction model is applicable to the present system consisting of amorphous-crystalline heterolayer structure. As is clear from Eq. (6), the magnitudes of N_I and V_D are graphically determined from the slope of the curve and the intercept on the horizontal axis, respectively, which are listed in Table I. Thus obtained values of N_I almost coincide with those determined independently from the low-frequency C-V measurement[24] on the Au/undoped a-Si:H/n^+ c-Si Schottky barrier diodes. The similar plot for the sample 3 (solid triangle) is also shown in the figure, which is deviated from a straight line. This apparent invalidity of Eq. (6) simply originates from a thinner undoped a-Si:H layer (0.8 μm thick). The depletion layer spreads over a whole a-Si:H (i.e., $W_2 = L$) when the reverse bias voltage exceeds some critical value, resulting in an upward break of the characteristic curve because much more fraction of reverse bias voltage is supported in p c-Si than expected from Eq. (4). Using the value of N_I obtained from the sample 7, the critical bias voltage at which W_2 reaches to L ($= 0.8$ μm) for the sample 3 was calculated as around -2 V, being in good agreement with the data in the figure.

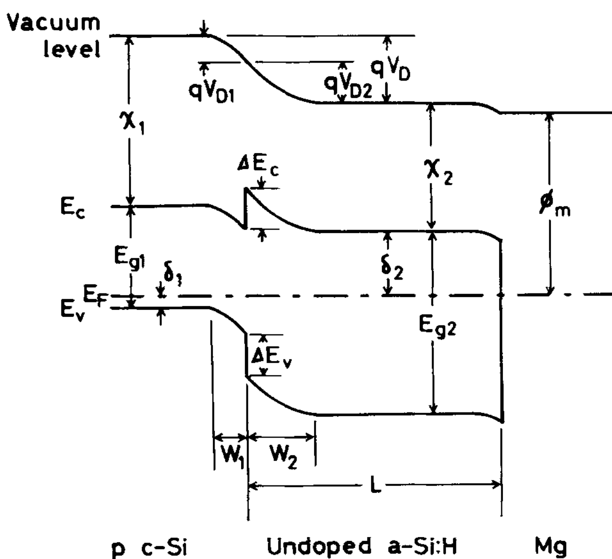

FIG. 3. Energy band diagram of p c-Si/undoped a-Si:H/Mg diode at equilibrium.

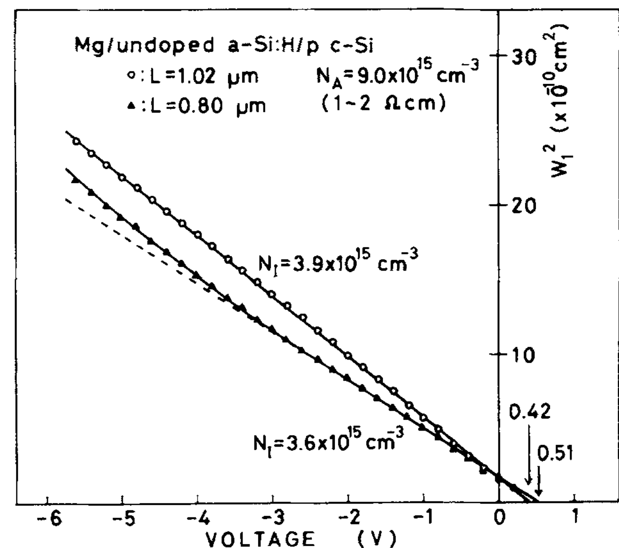

FIG. 4. Width of the depletion region in c-Si as a function of voltage for samples 3 ($L = 0.80$ μm) and 7 ($L = 1.02$ μm).

The electron affinity of a a-Si:H can be determined from the C-V characteristics of those heterojunctions. As is clear from the energy band diagram shown in Fig. 3, ΔE_C is expressed by

$$\Delta E_C = \delta_1 + \delta_2 - E_{g1} + qV_D, \tag{7}$$

as well as

$$\Delta E_C = \chi_1 - \chi_2. \tag{8}$$

By substituting quantitative data on δ_1, δ_2, χ_1, and V_D listed in the table to Eqs. (7) and (8), one can determine ΔE_C and χ_2. The obtained values of ΔE_C and χ_2 from each diode are also listed in the table. Although some statistical scatter is observed, the electron affinity (χ_2) of undoped a-Si:H is given as

$$\chi_2 = 3.93 \pm 0.07 \text{ eV}. \tag{9}$$

This value is coincident with the value of 3.93 eV within experimental margin of errors which was estimated[19] from the data of Yamamoto *et al.*[25] concerning internal photoemission experiment and the electron affinity of SiO_2.[26]

Figure 5 shows the energy band diagrams for each diode with different doping levels of p c-Si, sketched on the basis of the above results.

C. Current-voltage characteristics

J-V characteristics have been measured as a function of temperature in the range from 297–374 K, but the temperature range scanned in the present work is rather limited. Not only the band-like conduction but also hopping conduction like a variable-range hopping might prevail in the transport of a-Si:H at low temperatures although LeComber *et al.*[27] have reported that the nearest-neighbor hopping predominates below 240 K. Furthermore, the current density at 297 K decreases down to as low as 10^{-12} A/mm^2, causing another difficulty for measuring accurate junction properties.

Figures 6–9 show temperature dependence of J-V characteristics of Mg/undoped a-Si:H/p c-Si diodes, sample 5 ($\rho_{\text{cryst}} = 0.005$–$0.01\ \Omega$ cm), 6 ($\rho_{\text{cryst}} = 0.1$–$0.15\ \Omega$ cm), 7 ($\rho_{\text{cryst}} = 1$–$2\ \Omega$ cm), and 8 ($\rho_{\text{cryst}} = 5$–$10\ \Omega$ cm), respectively. Undoped a-Si:H films of 1.02 μm in thickness were deposited simultaneously on four different p c-Si substrates.

1. Forward J-V characteristics

According to any of the diffusion model,[15] the emission model,[16] and the recombination model,[28] a relation between J and V is represented by

$$J \propto \exp\left(\frac{qV}{\eta kT}\right), \tag{10}$$

where k is the Boltzmann's constant, T the measuring temperature, and η the diode factor being independent of temperature.

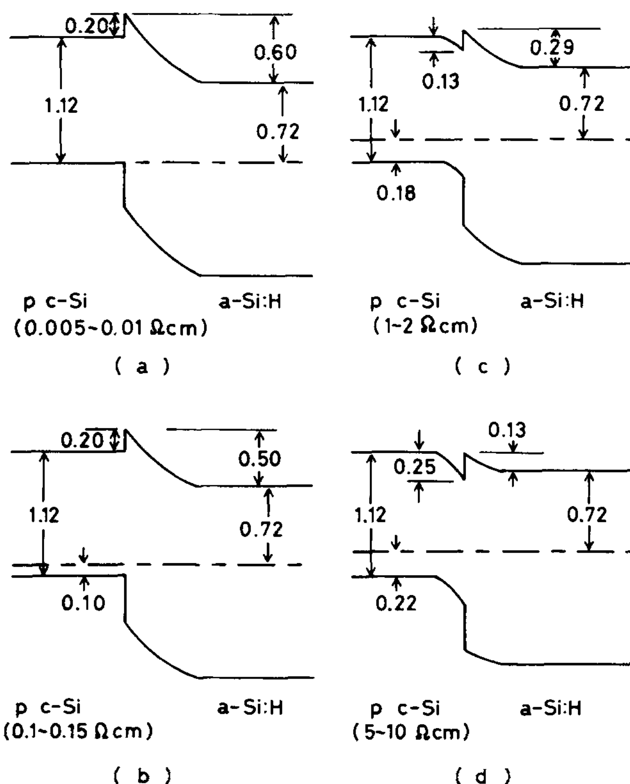

FIG. 5. Energy band diagrams in the interface region for heterojunctions using c-Si with four different resistivities.

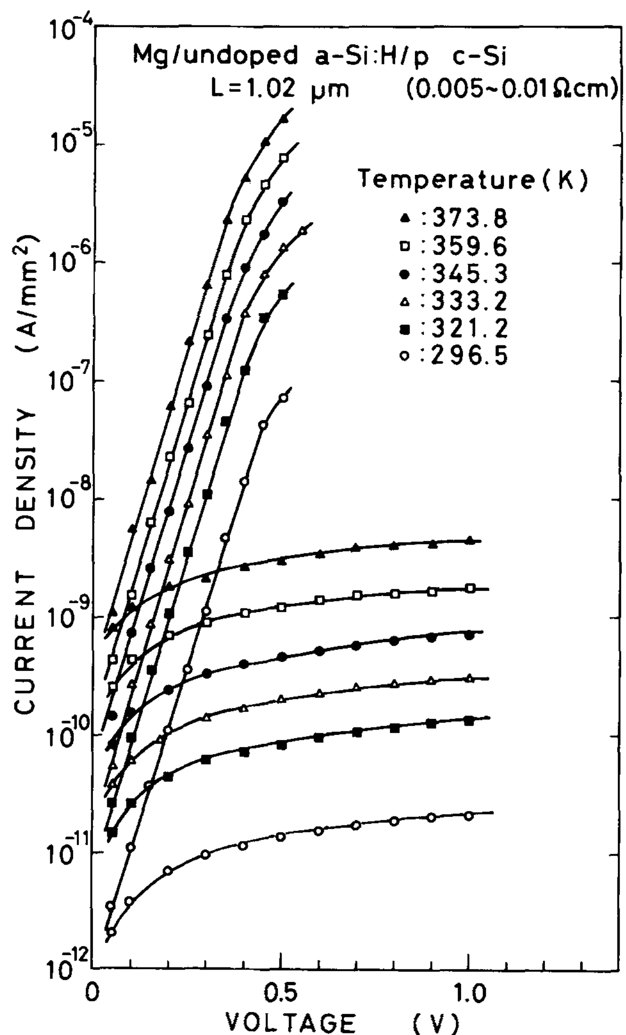

FIG. 6. J-V characteristics of sample 5 measured at six different temperatures.

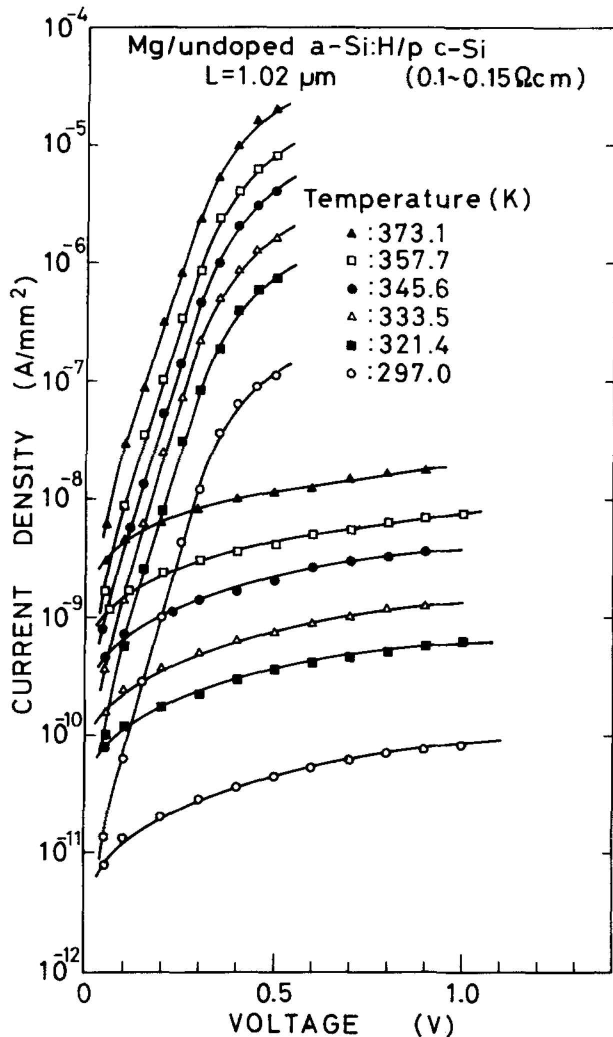

FIG. 7. J-V characteristics of sample 6 measured at six different temperatures.

As is clear from the results shown in the figure, a slope of the forward-bias curve is kept almost constant for varying temperatures, which indicates that Eq. (10) does not hold in the present system. Rather it suggests the transport phenomenon is limited by tunneling, being described as

$$J = J_0 \exp(AV), \tag{11}$$

where A is a temperature-independent constant. The data in Fig. 10 was analyzed using Eq. (11), resulting in the temperature dependence of the preexponential factor J_0 as shown in Fig. 10. Namely, the relation

$$J_0 \propto \exp\left(-\frac{\Delta E_{af}}{kT}\right), \tag{12}$$

holds between J_0 and T, where ΔE_{af} takes values of 0.72, 0.80, 0.65, and 0.63 eV for samples 5, 6, 7, and 8, respectively.

A variety of models for junction transport based on tunneling process have been proposed by several authors, [4,29] which are schematically shown in Fig. 11(a). For explaining the present experimental results, each model is examined one by one.

The simplest tunneling model consists of the tunneling of carriers through the spike-shaped barrier in the conduction band [Fig. 11(a)]. According to Riben *et al.*,[4] predominant tunnel flux takes place at an energy close to the peak of the barrier within an energy difference of about 0.1 eV for crystalline heterojunction, which is indicated by path "A" in the figure. In the present heterojunction, however, tunneling process at an energy range far below the barrier peak, indicated by path "B" in the figure, is quite possible because the localized states are quasi-continuously distributed within the gap of a-Si:H spatially as well as energetically. As is clear from the model, the magnitude of ΔE_{af} is expected to be smaller than value of V_{D2}. This requirement contradicts with the actual data, i.e., each experimentally obtained value of ΔE_{af} is larger than that of V_{D2}.

A second model is based on tunneling process of carriers, which has originally been presented for excess current in tunnel diodes.[30] As has been discussed by Riben *et al.*,[4,5] tunneling current by one-step tunneling [C or D in Fig. 11(a)] is always smaller than that by multitunneling (E in the figure). If we assume that their discussion can be applicable to

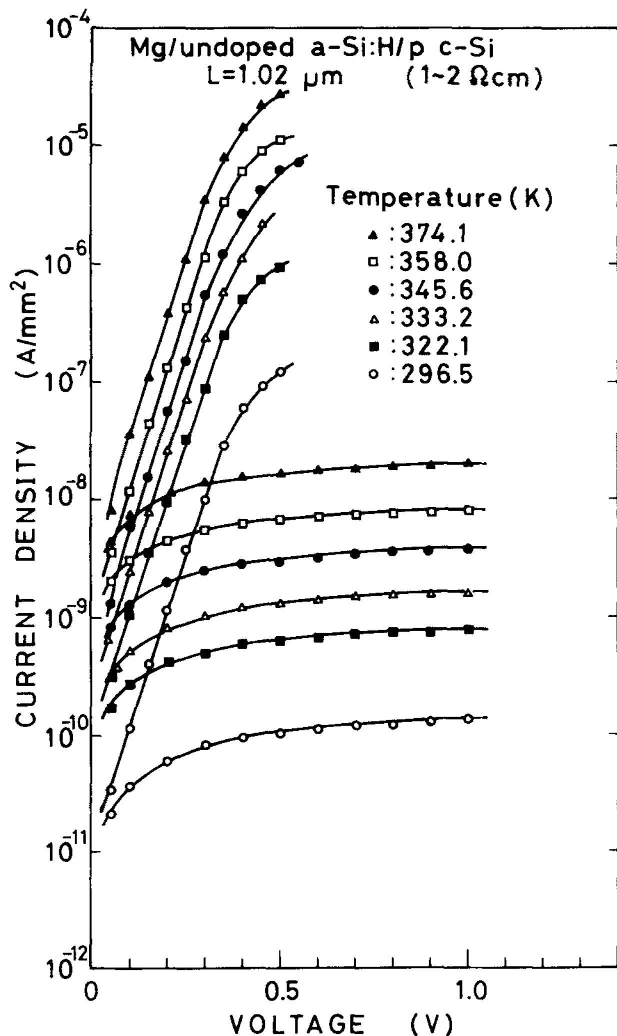

FIG. 8. J-V characteristics of sample 7 measured at six different temperatures.

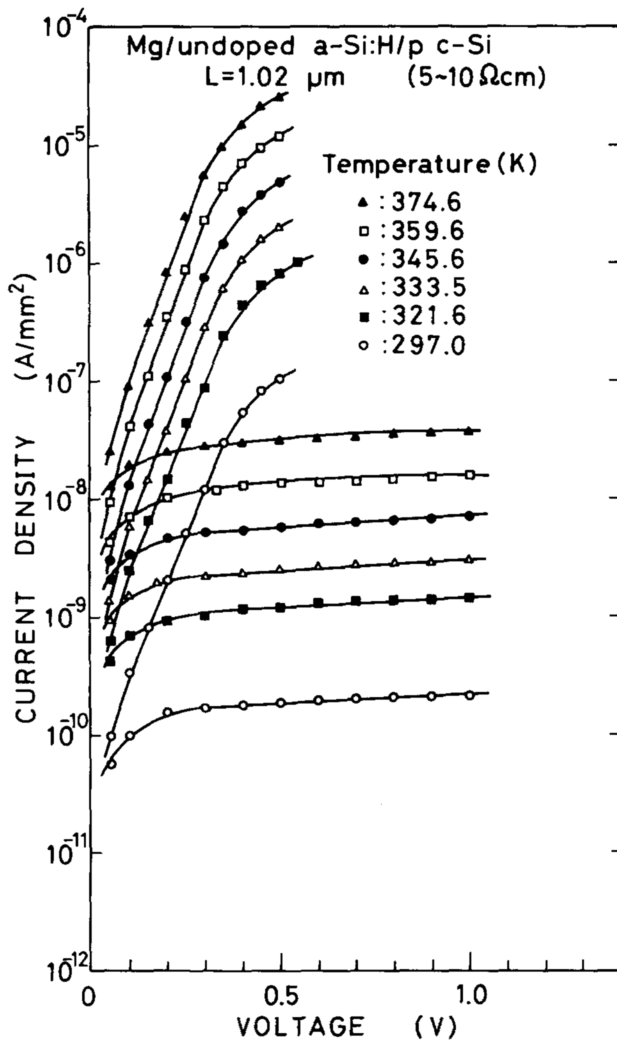

FIG. 9. J-V characteristics of sample 8 measured at six different temperatures.

the present a-Si:H junction, the multitunneling process should predominate in the present system since localized states are quasi-continuously distributed in the mobility gap. However, J_0 should change exponentially with T according to this multitunneling process,[4,5] while J_0 obtained in this study varies exponentially with $-1/T$ as shown in Fig. 10.

In order to solve this incoincidence, we propose the multitunneling capture-emission process as the most probable model for the present system, which is shown in Fig. 11(b). A hole in the valence band of p c-Si flows from one localized state to another in a-Si:H located within an energy range of kT by a multitunneling process and keeps flowing until a tunneling rate becomes smaller than the rate for hole release from the state to the valence band of a-Si:H or for recombination of the hole with an electron in the conduction band of a-Si:H. An ending point of tunneling might be close to the edge of the depletion layer of a-Si:H, where the tunneling rate decreases due to a decrease of electric field.

Thus, the current density flowing from p c-Si to the undoped a-Si:H is given by

$$J_{c\to a} = B(e_p + \sigma_n v_{th} n)\exp(AV), \tag{13}$$

where B is a constant independent of applied voltage and

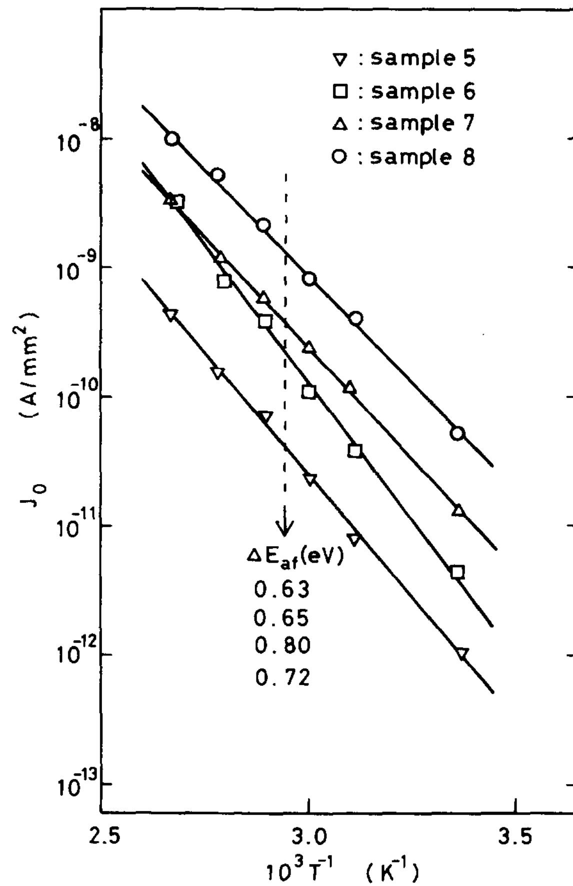

FIG. 10. Temperature dependence of the extrapolated values of J_0 of samples 5, 6, 7, and 8.

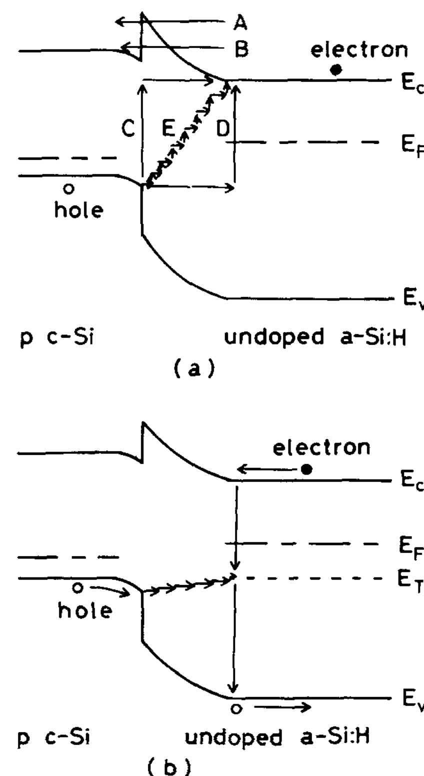

FIG. 11. Tunneling models for heterojunctions. (a) Reported tunneling models, (b) a multitunneling capture-emission model.

temperature, e_p the hole emission rate given as $e_p = \sigma_p v_{th} N_V \exp(-(E_T - E_V)/kT)$, σ_n the capture cross section of electrons, v_{th} the thermal velocity, n the electron density in the conduction band of a-Si:H given as $n = N_C \exp(-(E_C - E_F)/kT)$, σ_p the capture cross section of holes, N_V and N_C the effective densities of states in the valence band and the conduction band of a-Si:H, respectively, and E_F, E_T, E_V, and E_C, the energies of the Fermi level, trapping level, the valence band, and the conduction band of a-Si:H, respectively. Since no current flows in the diode when $V = 0$, the net current density is described as

$$J = J_0[\exp(AV) - 1], \tag{14}$$

$$J_0 = B\left[\sigma_p v_{th} N_V \exp\left(-\frac{E_T - E_V}{kT}\right) + \sigma_n v_{th} N_C \exp\left(-\frac{E_C - E_F}{kT}\right)\right]. \tag{15}$$

By comparing Eqs. (14) and (15) with the experimental data shown in Fig. 10, several possible comments can be deduced. For the junction property using the lowest-resistivity p c-Si (sample 5), $\Delta E_{af} = 0.72$ eV is obtained as shown in Fig. 10. This value coincides with that of the activation energy $\delta_2 (= E_C - E_F)$ of the dark conductivity of undoped a-Si:H. Therefore, considering from the band diagram shown in Fig. 5(a), the electron capture rate is larger than the hole emission rate, i.e., the second term predominates in the right-hand side of Eq. (15). On the other hand, for the samples 6, 7, and 8, obtained values of ΔE_{af} are 0.80, 0.65, and 0.63 eV, respectively, which is correlated with a decreasing tendency of the magnitude of $(E_T - E_V)$ with an increase in the substrate resistivity as shown in Fig. 5(b)–5(d). It suggested that hole emission prevails dominantly for these three samples, namely, the first term in the right-hand side of Eq. (15) determines the magnitude of J_0.

2. Reverse J-V characteristics

From Eq. (14), a saturated value of the reverse current density is expected to be J_0. However, as is clear from Figs. 6–9, the reverse current density (J_R) exceeds the value of J_0, indicating that the reverse current is limited by another transport mechanism. Furthermore, ΔE_{ar} of the reverse current at -0.1 V are 0.68, 0.70, 0.63, and 0.62 eV for the samples 5, 6, 7, and 8, respectively, which are different from ΔE_{af} for the forward bias characteristics.

Figure 12 shows the reverse current density plotted against $(V_D - V)^{1/2}$ for the samples 5 and 6, the diodes using lower-resistivity p c-Si substrates, the values of V_D is taken from Fig. 5. As shown in the figure. The reverse current is proportional to $(V_D - V)^{1/2}$ for two samples. It is noted that this proportionality holds in a whole temperature range studied in the present work. Since the bias voltage in these two diodes is mostly supported by the depletion layer of a-Si:H due to lower resistivity of p c-Si substrates, the reverse current is reasonably considered as a generation current from the obtained linear relationship between J_R and $(V_D - V)^{1/2}$.[31,32]

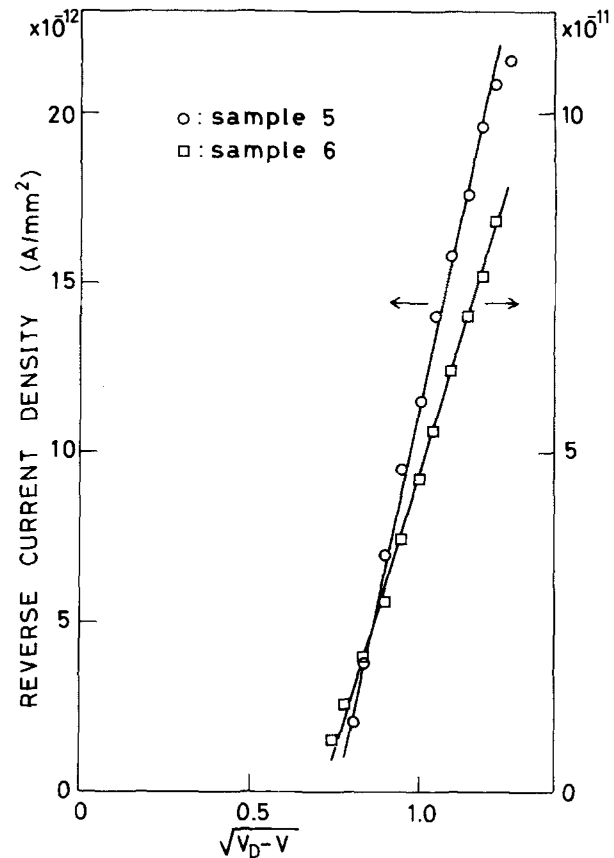

FIG. 12. Reverse current density-voltage characteristics of samples 5 and 6.

IV. SUMMARY

We have presented energy band diagrams for a-Si:H/c-Si heterojunctions on the basis of C-V characteristics of undoped (n^--type) a-Si:H heterojunctions formed on p-type c-Si substrates with four different resistivities. Also we have elucidated the current transport mechanism of these heterojunctions form J-V characteristics and their temperature dependence. The main results are summarized as follows:

(1) The high-frequency (100 kHz) C-V characteristics have been successfully analyzed of the heterojunctions with the high-resistivity undoped a-Si:H, from which it has been made clear that the abrupt heterojunction model is valid for a-Si:H/c-Si heterojunctions.

(2) The electron affinity of undoped a-Si:H has been estimated as 3.93 ± 0.07 eV from the diffusion voltage and the thermal activation energy of the dark conductivity of the undoped a-Si:H film, while the diffusion voltage is independently determined by C-V measurement.

(3) The forward current, described as $\exp(-\Delta E_{af}/kT) \times \exp(AV)$, can be explained by a multitunneling capture-emission model, where a hole in the valence band of p c-Si keeps flowing from one localized state to another in a-Si:H by a multitunneling process until its tunneling rate becomes smaller than a rate either for hole releasing from the state to the valence band or for its recombination with an electron in the conduction band of a-Si:H.

(4) The reverse current, described as $\exp(-\Delta E_{ar}/$

$kT) \times (V_D - V)^{1/2}$, has been reasonably ascribed to a generation current.

ACKNOWLEDGMENTS

We would like to thank A. Matsuda, H. Oheda, S. Yamasaki, and N. Hata for their fruitful discussion. We are also grateful to Dr. L. Malhotra and Dr. Y. Tokumaru for critical reading.

[1]R. L. Anderson, Solid-State Electron. **5**, 341 (1962).
[2]R. H. Rediker, S. Stopek, and J. H. R. Ward, Solid-State Electron. 7, 621 (1964).
[3]M. J. Hampshire and G. T. Wright, Br. J. Appl. Phys. **15**, 1331 (1964).
[4]A. R. Riben and D. L. Feucht, Solid-State Electron. **9**, 1055 (1966).
[5]A. R. Riben and D. L. Feucht, Int. J. Electron. **20**, 583 (1966).
[6]J. P. Donnelly and A. G. Milnes, Proc. IEEE **113**, 1468 (1966).
[7]W. Shockley, U.S. Patent 2,569,347 (1951).
[8]H. Kroemer, Proc. IRE **45**, 1535 (1957).
[9]R. H. Rediker, T. M. Quist, and B. Lax, Proc. IEEE **51**, 218 (1963).
[10]R. F. Rutz, Proc. IEEE **51**, 470 (1963).
[11]H. Kroemer, Proc. IEEE **51**, 1782 (1963).
[12]J. C. Marinace, IBM J. Res. Dev. **4**, 280 (1960).
[13]Y. Tawada, M. Kondo, H. Okamoto, and Y. Hamakawa, *Proc. 15th IEEE Photovoltaic Specialists Conf.*, Florida (1981), p. 245.
[14]S. S. Perlman and D. L. Feucht, J. Electron. **18**, 159 (1965).
[15]W. Shockley, *Electrons and Holes in Semiconductors* (Van Nostrand, Princeton, 1950), p. 309.
[16]E. Spenke, *Electronic Semiconductors* (McGraw-Hill, New York, 1958), p. 81.
[17]R. Grigorovici, N. Croitoru, A. Devenyi, and E. Teleman, *Proc. Int. Conf. Semiconductors, Paris 1964* (Academic Press, New York, 1964), p. 423.
[18]L. Štourač, *Proc. Int. Conf. Amorphous Semiconductors*, edited by R. Grigorovici and M. Ciurea, Bucharest 1982 (Central Institute of Physics, Bucharest, 1982), p. 104.
[19]H. Matsuura, T. Okuno, H. Okushi, S. Yamasaki, A. Matsuda, N. Hata, H. Oheda, and K. Tanaka, Jpn. J. Appl. Phys. **22**, L197 (1983).
[20]C. R. Wronski and D. E. Carlson, *Proc. 7th Int. Conf. Amorphous & Liquid Semiconductors*, edited by W. E. Spear, Edinburgh 1977 (CICI, Edinburgh, 1977), p. 452.
[21]T. Tiedje, C. R. Wronski, B. Abeles, and J. M. Cebulka, Solar Cells **2**, 301 (1980).
[22]D. V. Lang, J. D. Cohen, and J. P. Harbison, Phys. Rev. **B25**, 5285 (1982).
[23]A. G. Milnes and D. L. Feucht, *Heterojunctions and Metal-Semiconductor Junctions* (Academic, New York, 1972), p. 34.
[24]H. Okushi, K. Nakagawa, S. Yamasaki, H. Yamamoto, A. Matsuda, M. Matsumura, K. Tanaka, and S. Iizima, Jpn. J. Appl. Phys. **20**, Suppl. 20-2, 205 (1981).
[25]T. Yamamoto, Y. Mishima, M. Hirose, and Y. Osaka, Jpn. J. Appl. Phys. **20**, Suppl. 20-2, 185 (1981).
[26]S. M. Sze, *Physics of Semiconductor Devices* (Wiley-Interscience, New York, 1969), p. 468.
[27]P. G. LeComber and W. E. Spear, Phys. Rev. Lett. **25**, 509 (1970).
[28]S. M. Sze, *Physics of Semiconductor Devices* (Wiley-Interscience, New York, 1969), p. 104.
[29]A. G. Chynoweth, W. L. Feldmann, and R. A. Logan, Phys. Rev. **121**, 684 (1961).
[30]S. M. Sze, *Physics of Semiconductor Devices* (Wiley-Interscience, New York, 1969), p. 169.
[31]S. M. Sze, *Physics of Semiconductor Devices* (Wiley-Interscience, New York 1969), p. 103.
[32]Although the generation-recombination current should affect the forward current at low biases just as in *p-n c*-Si diodes, our data shown in Figs. 6–9 do not at least show this effect above 297 K. However, if *J-V* measurements are done below 297 K, this effect might appear in the forward current at low biases because ΔE_{af} is larger than ΔE_{ar}. It should be noted, however, that one should have difficulty for analyzing *J-V* characteristics originating from the change of transport mechanism in low T regime.
[33]S. M. Sze, *Physics of Semiconductor Devices* (Wiley-Interscience, New York, 1969), pp. 20, 38, 57, 468.